


RESEARCH ARTICLE

Open Access

Giant enhancement of nonlinear harmonics of an optical-tweezer phonon laser



Guangzong Xiao^{1,3*†} , Tengfang Kuang^{1,3†}, Yutong He^{1,3}, Xinlin Chen^{1,3}, Wei Xiong^{1,3}, Xiang Han^{1,3}, Zhongqi Tan^{1,3}, Hui Luo^{1,3*} and Hui Jing^{2*}

Abstract

Phonon lasers, as mechanical analogues of optical lasers, are unique tools for not only fundamental studies of the emerging field of phononics but also diverse applications such as deep-ocean monitoring, force sensing, and biomedical ultrasonics. Recently, nonlinear phonon-lasing effects were observed in an opto-levitated microsphere, i.e., the spontaneous emerging of weak signals of high-order phonon harmonics in the phonon lasing regime. However, both the strengths and the quality factors of the emerging phonon harmonics are very poor, thus severely hindering their potential applications in making and utilizing nonlinear phonon-laser devices. Here we show that, by applying a single-colour electronic injection to this levitated system, giant enhancement can be achieved for all higher-order phonon harmonics, with more than 3 orders enhanced brightness and 5 orders narrowed linewidth. Such an electronically-enhanced phonon laser is also far more stable, with frequency stability extended from a dozen of minutes to over 1 h. More importantly, higher-order phonon correlations, as an essential lasing feature, are confirmed to be enhanced by the electronic injection as well, which as far as we know, has not been reported in previous works using this technique. This work, providing much stronger and better-quality signals of coherent phonon harmonics, is a key step towards controlling and utilizing nonlinear phonon lasers for applications such as phonon frequency combs, broadband phonon sensors, and ultrasonic bio-medical diagnosis.

Keywords Phonon laser, Optomechanics, Optical tweezers

1 Introduction

The coherent generation and control of phonons are central to a variety of aspects of quantum metrology and quantum information science, including the development of quantum transducer [1–7], solid-state quantum computer [8–10], and metrological techniques for detecting gravitational wave or dark matter [11, 12]. Recent developments include the demonstration of phonon beam splitter [13], nonreciprocal sound devices [14, 15], topological mechanical lattice [16], and vibrational wave mixer [17], to name only a few. Phonon lasers, which is the mechanical analogues of optical lasers, characterized by a wavelength shorter than optical lasers of the same frequency [18], are expected to play a major role in driving phonon devices and improving force sensors [19], and thus great efforts have been devoted to realizing them with ions [20–23], micro-resonators [24–29], membrane

[†]Guangzong Xiao and Tengfang Kuang have contributed equally to this work.

*Correspondence:

Guangzong Xiao
xiaoguangzong@nudt.edu.cn

Hui Luo
luohui.luo@163.com

Hui Jing
jinghui@hunnu.edu.cn

¹ College of Advanced Interdisciplinary Studies, National University of Defense Technology, Changsha 410073, Hunan, China

² Department of Physics and Synergetic Innovation Center for Quantum Effects and Applications, Hunan Normal University, Changsha 410081, Hunan, China

³ Nanhu Laser Laboratory, National University of Defense Technology, Changsha 410073, Hunan, China

[30, 31], semi-conductor lattice [32], and photonic crystal [33]. These pioneering experiments on phonon laser, instead of thermal phonon amplification, have demonstrated three main features of any lasing: a threshold behaviour where the system switches from spontaneous to stimulated emissions [20], linewidth narrowing above the threshold [24, 34] and subthermal squeezing of phonons well characterized by the autocorrelations of $g^2(0) \sim 1$ [33–35], which proves the high order phonon coherence.

Recently, a nanosphere phonon laser operating in a levitated optomechanics (LOM) configuration was demonstrated [34], opening the door to exploring phononics with optical tweezers. However, it is highly challenging or even impossible to directly use the same way to realize phonon lasing for a micro-size object, since the dissipation of mechanical coupling can dominate due to strong scattering losses of the light. To overcome this difficulty, we introduce an optical gain into the cavity optomechanical system to compensate for the losses. Thus the dissipative coupling is significantly strengthened and the power threshold is suppressed. Then by using a levitated micro-size object, we demonstrated nonlinear multi-colour phonon lasers in an active LOM system, which features simultaneous emerging of weak higher-order mechanical harmonics, in addition to the fundamental-mode phonon laser [35]. Such nonlinear phonon lasers are potentially important for both fundamental studies of nonlinear phononics and diverse applications such as multi-mode phonon sensors or acoustic frequency combs [36].

However, due to strong dissipative couplings of the large-size objects with the light, nonlinear signals of higher-order harmonics in such levitated phonon-laser devices are typically very weak, thus severely hindering their applications in practice. We note that several methods have been presented previously to improve the quality of phonon lasers, such as feedback control [34], optical polarization control [32], and Floquet engineering [37]. Nevertheless, it has remained a highly nontrivial challenge to greatly improve the qualities of both the fundamental-mode phonon laser and all its higher-order harmonics for our levitated micro-sphere system till now. Here, for the first time, we show that by applying a simple but powerful way of electronic injection into our active LOM system, both the fundamental-mode phonon laser and all its higher-order harmonics can be well locked, leading to giant enhancement of their qualities, including brightness, linewidths, frequency stabilities, and higher-order coherence. Our work provides a significant step forward for enhancing and controlling micro-object phonon lasers, which can be highly desirable for a number of applications, especially for ultrasensitive metrology.

We note that injection locking, as a flexible tool to tune all kinds of oscillations [38–43], has been used to achieve

hertz-linewidth lasers [44–46], low-noise soliton micro-comb [47–49], and stable motion [50–53]. Particularly, for a trapped-ion system, this technique enabled 2 orders enhancements of phonon lasing brightness and linewidth narrowing, reaching a quality factor $Q_m \sim 10^4$, which was shown to be very useful for achieving ultrahigh force sensitivity [54]. However, as far as we know, there is no report about simultaneous locking of both fundamental-mode phonon laser and its higher-order harmonics, no report about locking-induced giant enhancement of nonlinear phonon harmonics, and more importantly, no report at all about its role in enhancing higher-order correlations of phonon lasers.

Here we confirm for the first time that not only the fundamental-mode phonon laser but also its nonlinear higher-order harmonics can be simultaneously enhanced by only a single-colour electronic signal. The new features of our present work are summarised as: (i) the brightness of the fundamental-mode phonon laser is enhanced by 3 orders of magnitude, compared to our previous work [35], with also 5 orders linewidth narrowing, reaching a quality factor $Q_m \sim 6.6 \times 10^6$ (which is 2 orders higher than those achieved with a cold ion system [54]); (ii) the frequency stability of the phonon laser is enhanced for 5 orders of magnitude, leading to a longer trapping lifetime of the micro-object, i.e., from 1.3 min to over 1.2 h; (iii) giant enhancement can also be observed for all the spontaneously emerging mechanical harmonics, which is not merely due to the locking, but the constructive interplay of the locking and the optical gain; (iv) for the first time, we identify the positive role of locking in enhancing the higher-order correlations of phonon lasers, which are actually the key features of lasing. With these advantages, we believe this active LOM system can serve as a powerful new tool to explore nonlinear optomechanical effects with different types of large-mass levitated objects, for potential diverse applications.

2 Results

For clear comparisons, we first consider the case without electronic control. As shown in Fig. 1a, by increasing the pump power P of the active cavity, the microsphere can be driven through a threshold from the thermal to the coherent phonon lasing regime, as also confirmed by phonon correlation function measurements discussed later in this paper. The inset of Fig. 1a shows the clear change of the phonon number distribution $p(n)$ from Boltzmann to the Gaussian. As also observed in the tweezer phonon laser of Ref. [34], we find that the variance of the distribution is clearly smaller than that of a thermal state with the same mean phonon number, a situation referred to as subthermal number squeezing, with a higher degree of squeezing leading to Poissonian

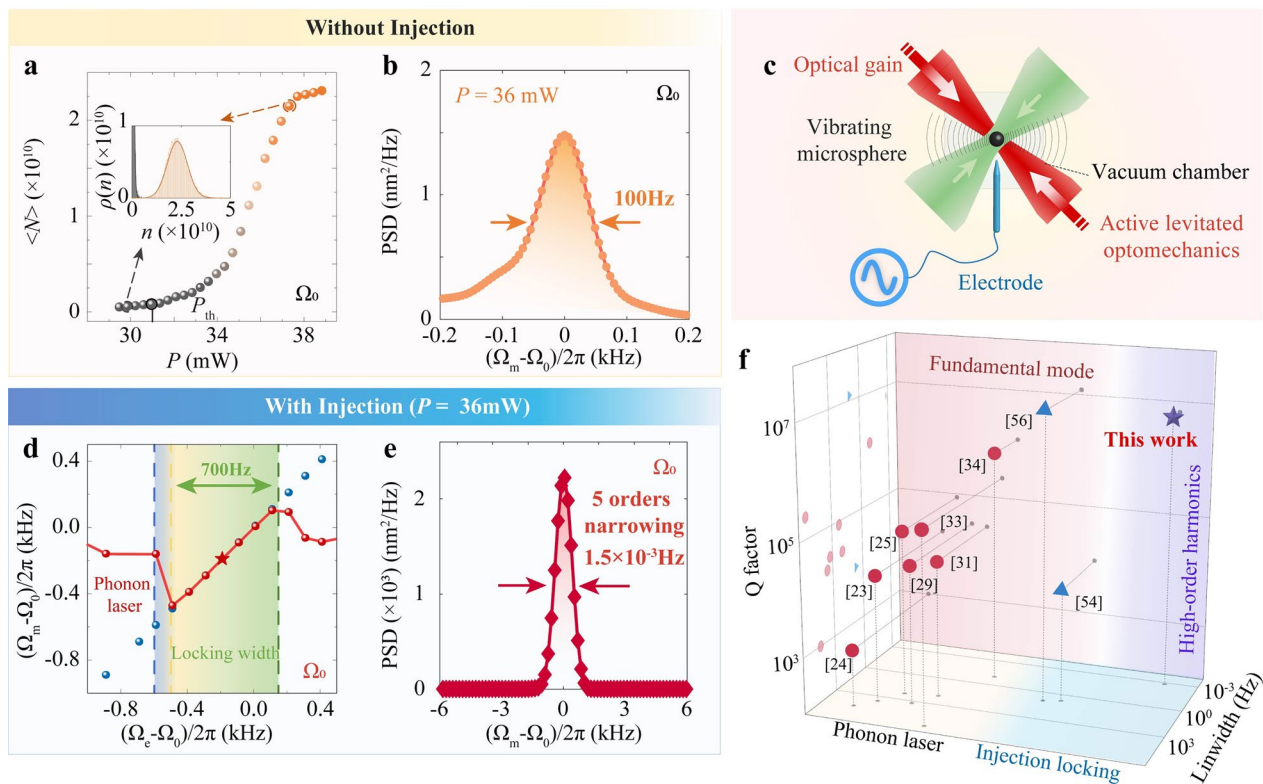


Fig. 1 Electronically-driven active LOM system with a micro-size sphere. **a** Phonon population $\langle N \rangle$ of the fundamental-mode phonon laser of frequency Ω_0 as a function of the laser pump power P . Inset: Phonon probability distributions below (grey) and above (coloured) the power threshold P_{th} . **b** Power spectral density (PSD) of the fundamental phonon laser mode above the threshold. **c** Schematic diagram of the experimental setup, including an active levitated optomechanics (red), a dual-beam optical tweezer (green), and an electrode (blue). **d** Measured phonon frequency as a function of the electronic frequency Ω_e , plotted over the locking width region. **e** PSD of the phonon laser when Ω_e falls within the locking width region (marked in **d**), showing a linewidth narrowing of 5 orders in comparison to the case without any injection, as shown in **(b)**. **f** A comparison of phonon lasers demonstrated till now, showing the advantage of our present work particularly in the quality factor and the linewidth. Also, except for our active LOM system, all the other phonon lasers only appear in the fundamental mode, i.e., without any nonlinear harmonics

statistics [34, 35]. The threshold of the fundamental phonon laser at Ω_0 is clearly apparent in the mean phonon population $\langle N \rangle = M\Omega_0 x^2 / \hbar$, with x its centre-of-mass displacement. Also, we observe that, below the threshold, the phonon mode linewidth is 2.5 kHz (for $P=30$ mW), and it is reduced to about 100 Hz for $P=36$ mW above the threshold (see Fig. 1b).

Our experimental system, as illustrated in Fig. 1c, consists of a dual-beam optical tweezer, a SiO_2 microsphere with mechanical frequency $\Omega_0=10.1$ kHz and an active optical gain medium pumped by a CW laser of power P [35] (see Supplementary Information for details). A tunable alternating current field of frequency Ω_e and amplitude U_e is applied to the microsphere. The distance d between the tip of the electrode and the trap centre is ~ 3 mm, and the natural charge q_e of the microsphere is measured as $2.35 \times 10^4 e$, estimated by $q_e = \langle F_{el} \rangle / E_e$, with [55]

$$F_{el} = \sqrt{\frac{S_x^{el}(\Omega)}{M^2[(\Omega^2 - \Omega_0^2)^2 + \Gamma_x^2 \Omega^2]}} \frac{2\tau \sin c^2[2(\Omega - \Omega_e)\tau]}{M^2[(\Omega^2 - \Omega_0^2)^2 + \Gamma_x^2 \Omega^2]} \quad (1)$$

where F_{el} is the electric force, $E_e = U_e/d$ the electric field intensity, M the mass of the microsphere, Γ_x the mechanical damping rate, τ the measurement time, and $S_x^{el}(\Omega)$ the power spectral density (PSD) value at the frequency Ω_e .

In our experiment, we scan Ω_e for a fixed $U_e=0.9$ V. The electronic force on the sphere is $\sim 4.47 \times 10^{-12}$ N, with a displacement amplitude of ~ 52 nm. The resulting shift $\Omega_m - \Omega_0$ clearly shows the locking of the phonon-laser frequency to Ω_e , as depicted in Fig. 1d. The locking width of this experiment is ~ 700 Hz. Compared with the unlocked system of Fig. 1b [35], we observe a 3 order of magnitude increase of the PSD and a 5 orders linewidth narrowing for the phonon laser, see Fig. 1e, with the

vibrating amplitude of the microsphere increased from ~ 127 nm to ~ 146 nm.

Compared with previous phonon lasers shown with different systems (e.g. micro-resonators [23–25, 29], vibrating membrane [31], optical lattice [33], nanomechanical devices [34, 54], or trapped ion [56]), our work indeed has advantages as given in Fig. 1f. The mechanical quality factor $Q_m = \Omega_m / \Gamma_m$ reaches 6.6×10^6 in this work. A higher quality factor was achievable for a levitated nanosphere (with a mass $\sim 10^{-18}$ kg), using sophisticated feedback controls based on electronic loops [56–58], which is difficult to apply for a micro-size sphere (with a mass $\sim 10^{-12}$ kg), due to much stronger scattering losses [59]. In our previous work, we used an optical gain to overcome this obstacle and achieve a microsphere phonon laser with a quality factor of ~ 400 [35], while this factor is improved here for 4 orders, reaching the highest record for this micro-object system. This ability, not achieved in previous works, can be important for applications requiring coherent control of a wide range of typical micro-size vibrating objects.

The frequency stability of our phonon laser can also be significantly improved, as shown in Fig. 2a. In the absence of any electronic control, the mechanical frequency drifts due to thermal noises and gain-induced heating [60], with a standard deviation of $\sigma \approx 1886.7$ Hz. This eventually leads to the escape of the sphere from the trap after ~ 13 min (see the grey dots). In contrast, for the present electronically-controlled system, the trapping lifetime of the microsphere can be increased to more than 1.2 h, with the standard deviation of the phonon frequency sharply falling down to $\sigma \approx 0.022$ Hz. That is, the relative standard deviation σ / Ω_0 is improved for 5 orders of magnitude, from 0.2 to 2×10^{-6} , a significant improvement compared to that achieved in Ref. [35]. Besides, compared with other works of injection locking [54, 56], neither work studies the effect of injection locking on stability, and has the data collection time less than 10 min actually. In contrast, we test the locked phonon laser for more than 1 h, and confirm that the frequency stability is enhanced significantly, which is a major breakthrough.

We emphasize that in contrast with previous works on injection locking of levitated oscillators [54, 56], in our present system, both the electronic injection and the optical gain are important. The giant enhancement of phonon lasers, as reported here, is not merely due to electronic locking. In fact, as demonstrated in Ref. [35], no significant multimode phonon lasing can be observed for a micro-size object in a passive LOM system. In contrast, clear evidence of multimode lasing is observed with an active cavity, a consequence of the gain-enhanced dissipative optomechanical coupling [35]. This fact is here confirmed by a series of measurements that apply only

the injection locking to the passive LOM system. This resulted in a weak peak at the locking frequency Ω_e , but none at the mechanical harmonics $n\Omega_e$, $n \geq 2$, see Fig. 2c.

We stress that the key to strongly enhancing the phonon lasers is the constructive interplay of two important factors, i.e., the electric locking and the optical gain, which is not straightforward to see at all. Indeed, this interplay can lead to not only the giant enhancement of the fundamental-mode phonon laser, but also the giant enhancement of all its higher-order harmonics. As shown in the grey curves of Fig. 2b, higher-order harmonics emerge spontaneously due to gain-enhanced LOM nonlinearity [35]. By applying the electric control, these harmonics can also be locked, resulting in 3 to 4 orders enhancement in the PSD. In addition, up to 8 high-order harmonics are observed, which have the potential to realize a high-quality phonon laser comb for a stronger nonlinearity. Compared with previous works about injection locking of phonon lasers [54, 56], this work is the first research on locking and giant enhancement of both the fundamental mode and the high-order harmonics of phonon lasers. In the work of trapped-ion phonon laser [54], electronic injection enabled 2 orders enhancements of both fundamental-mode lasing brightness and linewidth narrowing. In the work of nanoparticle phonon laser [56], electronic injection enabled 2 orders enhancement of fundamental-mode lasing brightness and 1 order enhancement of linewidth narrowing. In our work, the brightness of the fundamental-mode phonon laser is enhanced by 3 orders of magnitude, which is 1 order greater than the work mentioned above. Besides, the linewidth in our work is 3 orders narrowed relatively.

Furthermore, this is clearly different from a previous experiment in which a signal close to mechanical harmonic or subharmonic frequencies was injected into a microtoroidal optomechanical oscillator [50] and then resulted in only the locking of the fundamental mode. As such, our results represent a significant advance from that work since here in the nonlinear regime, both the fundamental phonon-laser mode and all its higher-order harmonics can be simultaneously locked, resulting in giant enhancement of otherwise very weak nonlinear harmonics, by applying only a single-colour signal. Also, we remark that our work is clearly different from the recent one on microcavity phononitons [61], which applied an electronic signal to an acoustic resonator to generate driving phonons, with strict frequency-matching conditions in their dispersive system.

Importantly, as shown in Fig. 2d and e, the linewidths of all mechanical harmonics of the phonon laser are also very significantly improved by the injection locking: In the absence of any injection, the linewidths of the second and third order harmonics at $2\Omega_0$ and $3\Omega_0$

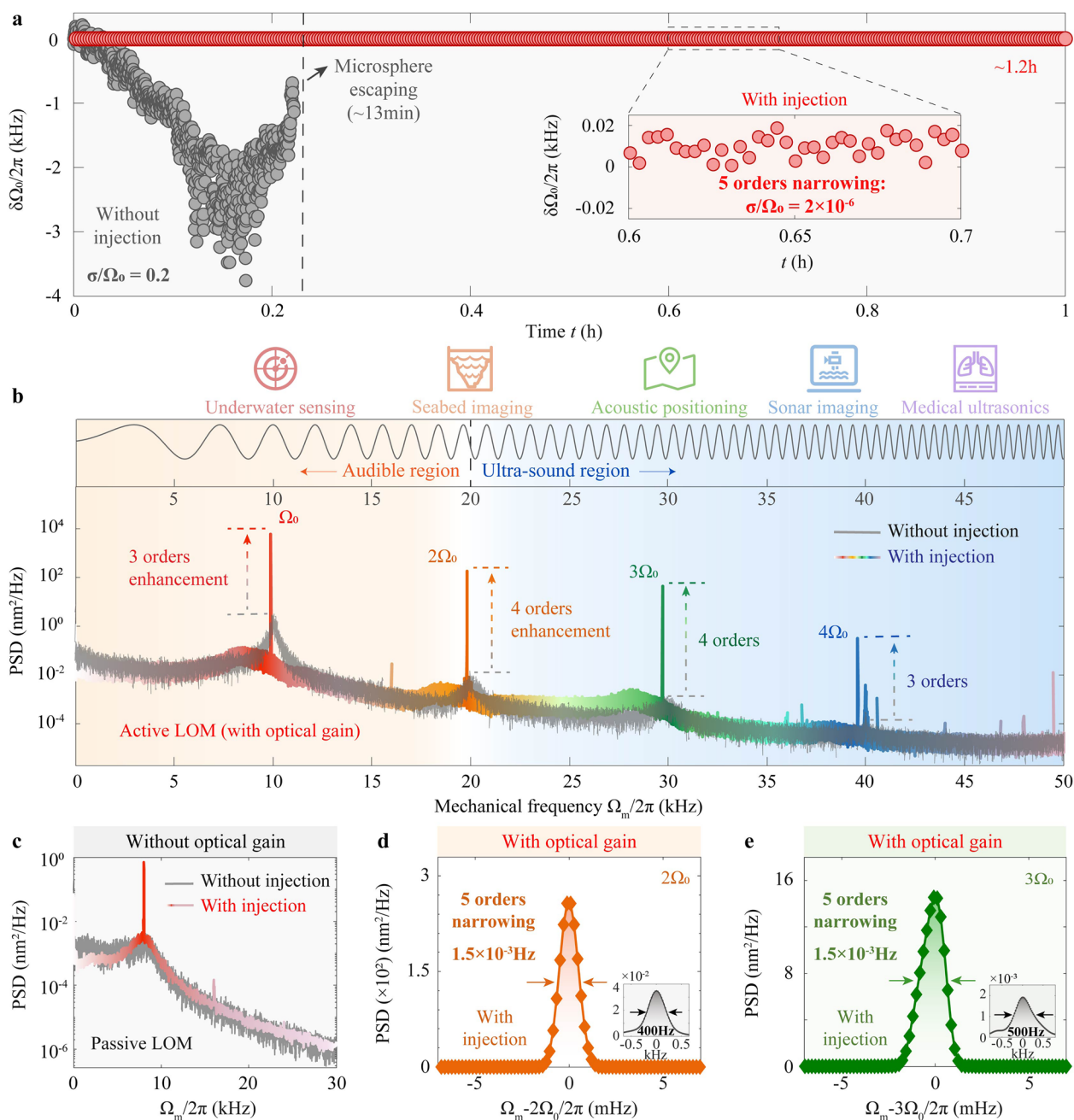


Fig. 2 Comparison of nonlinear phonon lasers for locked and unlocked conditions. **a** Mechanical frequency stabilities for the unlocked case (grey) and locked case (red). The inset shows a detailed view of the corresponding curve. σ/Ω_0 : Relative standard deviation, where σ is the standard deviation of the mechanical frequency. **b** The measured PSD of phonons in the active LOM system for the case without (grey) or with (coloured) the injection. The typical application of this work is above covering both the ranges of audible region and ultra-sound region. **c** The PSD for a passive LOM system without optical gain. **d, e** The detailed PSDs of the double-frequency mode $2\Omega_0$ and the triple-frequency mode $3\Omega_0$. Insets: The PSDs for the case without any electronic control

are about 400 Hz and 500 Hz, respectively, and the electronic injection reduces them by about 5 orders of magnitude, corresponding to mechanical quality factors of 1.32×10^7 and 1.98×10^7 , respectively. This giant

improvement of high-order harmonics is conducive to the application of phonon laser in more scenes. As demonstrated in Fig. 2b, the fundamental phonon laser, whose frequency (~ 10 kHz) falls within the audible

region, has no advantage for ultrasonic applications. In sharp contrast, the high-order phonon sidebands, such as the quadruple frequency sideband of about 40 kHz whose brightness is improved for 3 orders, obviously enter the ultra-sound region and thus have unique advantages in applications such as sonar imaging and biomedical ultra-sonics.

Finally, in order to confirm the coherent nature of phonon modes in our present system, we carried out a method to reveal the locking impact on the higher-order coherence of the phonon lasers by measuring the phonon field autocorrelations functions at zero-time delay [62], $g^{(k)}(0) = \langle \hat{b}^{\dagger k} \hat{b}^k \rangle / \langle \hat{b}^{\dagger} \hat{b} \rangle^k$, $k = 2, 3, 4$, with \hat{b} and \hat{b}^{\dagger} the annihilation and creation operators of the mechanical mode, with

$$g^{(2)}(0) = \frac{\langle \hat{N}^2 \rangle - \langle \hat{N} \rangle^2}{\langle \hat{N} \rangle^2}, \tag{2}$$

$$g^{(3)}(0) = \frac{1}{\langle \hat{N} \rangle^3} (\langle \hat{N}^3 \rangle - 3\langle \hat{N} \rangle^2 + 2\langle \hat{N} \rangle), \tag{3}$$

$$g^{(4)}(0) = \frac{1}{\langle \hat{N} \rangle^4} (\langle \hat{N}^4 \rangle - 6\langle \hat{N} \rangle^3 + 11\langle \hat{N} \rangle^2 - 6\langle \hat{N} \rangle), \tag{4}$$

and \hat{N} is the mean phonon number in the mode under consideration. Such studies, as far as we know, have not been reported previously using the injection techniques.

To analyse the impact of the injected signal on the coherence of the phonon laser, we measure $g^{(k)}(0)$ as shown in Fig. 3. In the absence of locking, as the pump power P exceeds the threshold, $g^{(k)}(0)$ of both the fundamental and first harmonic modes decreases to approach 1, see the left region in Fig. 3a and b. However, $g^{(k)}(0)$ falls short of 1, due to thermal motion [35]. We note that the locking has the advantage of noise suppressing and thus enhances the coherence, as the right region in Fig. 3a. With the injection voltage increases, $g^{(k)}(0)$ approaches 1 closer, demonstrating a stronger coherent state. Typically, $g^{(2)}(0)$, $g^{(3)}(0)$ and $g^{(4)}(0)$ falls to 1.04, 1.12 and 1.26, respectively. Similar results are also observed for double frequency component $2\Omega_0$ (see the right region in Fig. 3b), where $g^{(2)}(0)$, $g^{(3)}(0)$ and $g^{(4)}(0)$ decrease to 1.06, 1.20 and 1.49. In addition, we compare the phonon

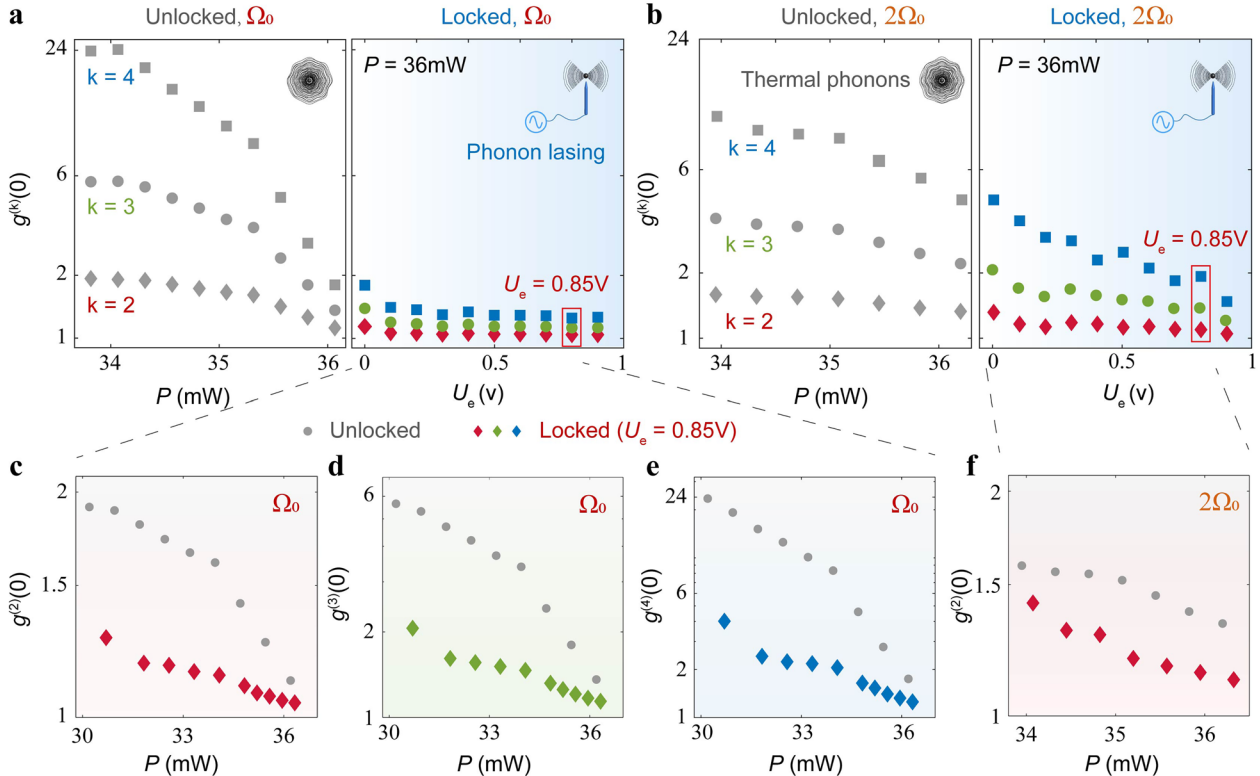


Fig. 3 Phonon correlations for unlocked (grey) and locked (coloured) LOM systems. **a, b** The autocorrelations at zero-time delay, $g^{(k)}(0)$, versus pump power P and U_e for Ω_0 and $2\Omega_0$. **c** Second-order autocorrelations at zero-time delay, $g^{(2)}(0)$, versus pump power P for Ω_0 . **d, e** Third or fourth order autocorrelations, $g^{(3)}(0)$ and $g^{(4)}(0)$, for Ω_0 . **f** $g^{(2)}(0)$ for $2\Omega_0$

coherence with or without locking, as demonstrated in Fig. 3c and f. We find that when applying the injection, $g^{(2)}(0)$ approaches $g^{(2)}(0)=1$ more rapidly, with a lower value than the case without locking, for the same driving. Similar results also can be observed for $g^{(3)}(0)$ and $g^{(4)}(0)$, see Figs. 3d and e for specific examples.

These results, to the best of our knowledge, have not been reported so far for phonon lasers (and even optical lasers), and clearly evidence the role of injection in improving high-order lasing coherence. We expect that such effects can be observed also in other phonon-laser devices using e.g., cold ions, vibrating membranes, and semiconductor lattices [20–33]. We stress that, although the three key ingredients of our experiment, i.e., the optical tweezer, the electronic locking, and the active gain, are well-established techniques, their marriage for engineering nonlinear phonon harmonics and enhancing their higher-order coherence has not been demonstrated in previous works. In fact, the advantage of this marriage is seen not only in Fig. 1, through detailed comparisons of our work with previous ones, but also in Figs. 2 and 3, confirming its remarkable role in enhancing nonlinear harmonics and more importantly, their high-order correlations. In contrast to the fundamental-mode phonon laser, these harmonics are well beyond the audible region and hence can be potentially useful for high-frequency applications as e.g., ultrasound material tests or biomedical diagnosis. In our future work, by further combining with other nonlinear processes, it is also possible to build coherent phonon frequency comb with uniform comb teeth and longer lifetime [63], a novel possibility as already demonstrated very recently in a purely optical system [64].

3 Conclusion

In summary, by the direct application of electronic injection locking into an active LOM system, we have demonstrated a considerable improvement in several key features of multi-mode phonon lasers with a micro-size sphere. We found that an effective locking of both the fundamental mode and its higher-order mechanical harmonics is achieved, with three orders of magnitude brighter and five orders of magnitude narrower linewidth, corresponding to mechanical quality factors of more than $Q_m = 10^6$. We also demonstrated that, for the same driving strength, higher-order phonon correlations approach unity more rapidly than the case without any electronic injection. Such a positive role in enhancing higher-order coherence, as far as we know, has not been reported for injection-locked phonon lasers (or even optical lasers).

As the final remark, we note that in previous experiments [51, 56], the locking signals were generated

optically and transformed into electronic signals through an electro-to-optical modulator. In contrast, in our work, the input signal is applied directly from an electrode, free of additional conversion devices, reducing the rigorous requirements on input sources. With this approach, we obtain the highest quality factor reported so far for the phonon laser, with also giant enhancement of the nonlinear phonon harmonics. This electro-LOM system offers a promising platform to explore nonlinear phononics and to build truly coherent acoustic frequency comb [36]. Besides, it is promising to realize spatial separated multiple phonon lasers by levitating two or more microspheres in our system, and study their synchronization characteristics [65, 66], collective many-body effects and even entangled phonon lasers or distributed coherent force sensors [67]. Future works will also investigate other novel possibilities such as achieving squeezed phonon lasers, and consider their applications in quantum metrology [68, 69].

4 Materials and methods

4.1 Experimental details

The experimental setup consists of four parts, including an active levitated optomechanical system, a dual-beam optical tweezer, electronic injection devices and a position detection system. As shown in Fig. 1c, the active levitated optomechanics is vertical to the dual-beam optical tweezer around the trapping region. The active levitated optomechanics is composed of a fibre laser path (with optical gain) and a free-space laser path. We install the free-space laser path of the active cavity to a 3D translation stage. Then, the relative position of the active cavity to the trapped microsphere is tuned with a resolution of 0.1 μm . The detailed parameter is also found in Ref. [35]. We apply electronic injection to the trapped microsphere through an electrode, which is installed directly below the microsphere in the direction of gravity. It is made of polished stainless steel with a tip radius of 200 μm . The distance d_0 between the trap centre and the electrode is measured to be about 3 mm. A function signal generator (DG1402-8750) is installed to generate the electronic field, and then a tunable alternating current (AC) field could be applied to the microsphere.

4.2 Experimental procedure

The experiment is mainly operated with the following three steps. (i) Microsphere trapping. Microspheres are loaded into the trapping region with a nebulizer. In most cases, a microsphere is trapped within 30 s. Once a microsphere is trapped, we switch on the vacuum pump

system and reduce the pressure to the desired level. (ii) Phonon lasing. The free-space laser path of the active cavity is installed on a 3D translation stage. We adjust its relative position to the microsphere in order to optimize the dissipative coupling strength. The phonon lasing behaviour is observed, according to the real-time PSD of the microsphere's displacement. (iii) Electronic injection and data acquisition. We adjust the amplitude and frequency of the signal generator according to the phonon lasing dynamic. Then, we investigate the influence of the electronic injection on the characteristics of the fundamental mode phonon laser and its high-order harmonics, as shown in the main text.

4.3 Charge estimation

The natural charge of q_e of the microsphere is estimated by $q_e = \langle F_{el} \rangle / E_e$, with the relationship $F_{el} = \sqrt{S_x^{el}(\Omega) / \frac{2\tau \sin^2 c^2 [2(\Omega - \Omega_e)\tau]}{M^2[(\Omega^2 - \Omega_e^2)^2 + \Gamma_x^2 \Omega^2]}}$. The equation comes from the Langevin equation of the microsphere, which can be expressed as $m\ddot{x} + m\Gamma_x \dot{x} + kx = F_{th}(x) + F_{el}(t)$, where $F_{el}(t) = F_{el-x} \cos(\omega_{dr}t)$. Then, the power density of the microsphere can be calculated as $S_x^{el}(\omega) = \frac{S_{v_x}^{el}(\omega)}{\beta^2} = \frac{2F_{el-x}^2 \tau \sin^2 c^2 [2(\omega - \omega_{dr})\tau]}{m^2[(\omega^2 - \omega_x^2)^2 + \Gamma_x^2 \omega^2]}$. In the experiment, we get the PSD from the displacement of the microsphere. As the sphere alters the spatial distribution of the scattering light, the differential mode signal from the BPD reveals the sphere's position. With the electric force in hand, we can estimate the natural charge q_e . Here, we approximate the electric field strength to the strength of the input electrical signal, and then for a single suspended microsphere the charge can be calculated.

Supplementary Information

The online version contains supplementary material available at <https://doi.org/10.1186/s43593-024-00064-8>.

Supplementary Material 1.

Acknowledgements

We sincerely thank Prof. Pierre Meystre at the University of Arizona for many insightful discussions and suggestions about this work. The new findings of this work, after posting on arXiv, were reported by New Scientist (entitled: 'Sound laser' is the most powerful ever made [70]).

Author contributions

G.X. and H.J. conceived the idea. G.X. and T.K. designed the experiments. T.K. and Y.H. performed the experiments and analyzed the experimental data with the help of X.C., W.X. and X.H. T.K. and Y.H. wrote the manuscript with contributions from G.X. and H.J. Z.T., H. L. and H. J. supported the project.

Funding

G.X. is supported by Fund for Distinguished Young Scholars of Hunan Province (2024JJ2055). H.J. is supported by the NSFC (11935006), the Science and

Technology Innovation Program of Hunan Province (Grant No. 2020RC4047), National Key R&D Program of China (No. 2024YFE0102400) and Hunan provincial major sci-tech program (2023ZJ1010).

Availability of data and materials

All data needed to evaluate the conclusions in the paper are present in the paper and supporting information. Additional data related to this paper may be requested from the authors.

Declarations

Ethics approval and consent to participate

Not applicable.

Consent for publication

Not applicable.

Competing interests

The authors declare no competing interests.

Received: 26 March 2024 Revised: 21 April 2024 Accepted: 8 May 2024

Published online: 05 September 2024

References

1. R. Andrews et al., Bidirectional and efficient conversion between microwave and optical light. *Nat. Phys.* **10**(4), 321–326 (2014)
2. M. Mirhosseini, A. Sipahigil, M. Kalaei, O.J. Painter, Superconducting qubit to optical photon transduction. *Nature* **588**(7839), 599–603 (2020)
3. W. Jiang et al., Efficient bidirectional piezo-optomechanical transduction between microwave and optical frequency. *Nat. Commun.* **11**(1166), 1–7 (2020)
4. K. Stannigel, P. Rabl, A.S. Sørensen, P. Zoller, M.D. Lukin, Optomechanical transducers for long-distance quantum communication. *Phys. Rev. Lett.* **105**(22), 220501 (2010)
5. J.T. Hill, A.H. Safavi-Naeini, J. Chan, O.J. Painter, Coherent optical wavelength conversion via cavity optomechanics. *Nat. Commun.* **3**(11), 1196 (2012)
6. T.A. Palomaki et al., Coherent state transfer between itinerant microwave fields and a mechanical oscillator. *Nature* **495**(7440), 210–214 (2013)
7. X. Zhang, C. Zou, L. Jiang, H.X. Tang, Strongly coupled magnons and cavity microwave photons. *Phys. Rev. Lett.* **113**(15), 156401 (2014)
8. R. Manenti et al., Circuit quantum acoustodynamics with surface acoustic waves. *Nat. Commun.* **8**(1), 975 (2017)
9. Y. Chu et al., Quantum acoustics with superconducting qubits. *Science* **358**(6360), 199–202 (2017)
10. K.J. Satzinger et al., Quantum control of surface acoustic-wave phonons. *Nature* **563**(7733), 661–665 (2018)
11. B.P. Abbott et al., Observation of gravitational waves from a binary black hole merger. *Phys. Rev. Lett.* **116**(6), 061102 (2016)
12. H. Grote et al., Direct limits for scalar field dark matter from a gravitational-wave detector. *Nature* **600**(7889), 424–428 (2021)
13. H. Qiao et al., Splitting phonons: building a platform for linear mechanical quantum computing. *Science* **380**(6649), 1030–1033 (2023)
14. T. Nomura et al., Nonreciprocal phonon propagation in a metallic chiral magnet. *Phys. Rev. Lett.* **130**(17), 176301 (2023)
15. Z. Shen et al., Reconfigurable optomechanical circulator and directional amplifier. *Nat. Commun.* **9**(1), 1797 (2018)
16. J. Cha, K.W. Kim, C. Daraio, Experimental realization of on-chip topological nanoelectromechanical metamaterials. *Nature* **564**(7735), 229–233 (2018)
17. M. Kurosu, D. Hatanaka, K. Onomitsu, H. Yamaguchi, On-chip temporal focusing of elastic waves in a phononic crystal waveguide. *Nat. Commun.* **9**(1), 1–7 (2018)
18. R. Huang, H. Jing, The nanosphere phonon laser. *Nat. Photonics* **13**(6), 372–373 (2019)
19. K. Cui et al., Phonon lasing in a hetero optomechanical crystal cavity. *Photonics Res.* **9**(6), 937–943 (2021)

20. K.J. Vahala et al., A phonon laser. *Nat. Phys.* **5**(9), 682–686 (2009)
21. T. Behrle et al., Phonon laser in the quantum regime. *Phys. Rev. Lett.* **131**(4), 043605 (2023)
22. C. Lee, K. Lin, G. Lin, Prototype of a phonon laser with trapped ions. *Phys. Rev. Res.* **5**(2), 023082 (2023)
23. Y. Wei et al., Detection of DC electric forces with zeptonewton sensitivity by single-ion phonon laser. *Sci China Phys Mech* **65**(11), 111–118 (2022)
24. I.S. Grudinin, H. Lee, O. Painter, K.J. Vahala, Phonon laser action in a tunable two-level system. *Phys. Rev. Lett.* **104**(8), 083901 (2010)
25. J. Zhang et al., A phonon laser operating at an exceptional point. *Nat. Photonics* **12**(8), 479–484 (2018)
26. G. Wang et al., Demonstration of an ultra- low-threshold phonon laser with coupled microtoroid resonators in vacuum. *Photonics Res.* **5**(2), 73–76 (2017)
27. H. Jing et al., PT-symmetric phonon laser. *Phys. Rev. Lett.* **113**(5), 053604 (2014)
28. Y. Jiang, S. Maayani, T. Carmon, F. Nori, H. Jing, Nonreciprocal phonon laser. *Phys. Rev. Appl.* **10**(6), 064037 (2018)
29. N. Wang et al., Laser²: a two-domain photon-phonon laser. *Sci. Adv.* **9**(26), eadg7841 (2023)
30. U. Kemiktarak, M. Durand, M. Metcalfe, J. Lawall, Mode competition and anomalous cooling in a multimode phonon laser. *Phys. Rev. Lett.* **113**(3), 030802 (2014)
31. Q. Zhang, C. Yang, J. Sheng, H. Wu, Dissipative coupling-induced phonon lasing. *Proc. Natl. Acad. Sci. U.S.A.* **119**(52), e2207543119 (2022)
32. D.L. Chafatinos et al., Polariton-driven phonon laser. *Nat. Commun.* **11**(1), 1–8 (2020)
33. J.D. Cohen et al., Phonon counting and intensity interferometry of a nanomechanical resonator. *Nature* **520**(7548), 522–525 (2015)
34. R.M. Pettit et al., An optical tweezer phonon laser. *Nat. Photonics* **13**(6), 402–405 (2019)
35. T. Kuang et al., Nonlinear multi-frequency phonon lasers with active levitated optomechanics. *Nat. Phys.* **19**(3), 414–419 (2023)
36. M.H.J. de Jong, A. Ganesan, A. Cupertino, S. Groblacher, R.A. Norte, Mechanical overtone frequency combs. *Nat. Commun.* **14**(1), 1458 (2023)
37. L. Mercade et al., Floquet phonon lasing in multimode optomechanical systems. *Phys. Rev. Lett.* **127**(7), 073601 (2021)
38. R. Adler, A study of locking phenomena in oscillators. *Proc. IRE* **34**(6), 351–357 (1946)
39. L. Paciorek, Injection locking of oscillators. *Proc. IEEE* **53**(11), 1723–1727 (1965)
40. B. Razavi, A study of injection locking and pulling in oscillators. *IEEE J. Solid-State Circuits* **39**(9), 1415–1424 (2004)
41. W.H. Steier, H.L. Stover, Locking of laser oscillators by light injection. *IEEE J. Quantum Electron.* **2**(4), 111–112 (1966)
42. Z. Liu, R. Slavík, Optical injection locking: from principle to applications. *J. Lightwave Technol.* **38**(1), 43–59 (2020)
43. N.M. Kondratiev et al., Recent advances in laser self-injection locking to high-Q microresonators. *Front. Phys.* **18**(2), 1–42 (2023)
44. W. Liang et al., Ultralow noise miniature external cavity semiconductor laser. *Nat. Commun.* **6**(7371), 1–6 (2015)
45. W. Jin et al., Hertz-linewidth semiconductor lasers using cmos-ready ultra-high-Q microresonators. *Nat. Photonics* **15**(5), 346–353 (2021)
46. C. Xiang et al., 3d integration enables ultralow-noise isolator-free lasers in silicon photonics. *Nature* **620**(7972), 78–85 (2023)
47. N.G. Pavlov et al., Narrow-linewidth lasing and soliton kerr microcombs with ordinary laser diodes. *Nat. Photonics* **12**(11), 694–698 (2018)
48. G. Lihachev et al., Platicon microcomb generation using laser self- injection locking. *Nat. Commun.* **13**(1), 1771 (2022)
49. A.S. Voloshin et al., Dynamics of soliton self-injection locking in optical microresonators. *Nat. Commun.* **12**(1), 235 (2021)
50. M. HosseinZadeh, K.J. Vahala, Observation of injection locking in an optomechanical rf oscillator. *Appl. Phys. Lett.* **93**(19), 191115 (2008)
51. S. Kuhn et al., Optically driven ultra-stable nanomechanical rotor. *Nat. Commun.* **8**(1), 1–5 (2017)
52. C.J. Bekker, R. Kalra, C.G. Baker, W.P. Bowen, Injection locking of an electro-optomechanical device. *Optica* **4**(10), 1196–1204 (2017)
53. G. Arregui et al., Injection locking in an optomechanical coherent phonon source. *Nanophotonics* **10**(4), 1319–1327 (2021)
54. S. Knünz et al., Injection locking of a trapped-ion phonon laser. *Phys. Rev. Lett.* **105**(1), 013004 (2010)
55. S. Zhu et al., Nanoscale electric field sensing using a levitated nano-resonator with net charge. *Photonics Res.* **11**(2), 279–289 (2023)
56. S. Dadras et al., Injection locking of a levitated optomechanical oscillator for precision force sensing. 2020. <https://arxiv.org/abs/2012.12354>
57. Y. Zheng, L. Liu, X. Chen, G. Guo, F. Sun, Arbitrary nonequilibrium steady-state construction with a levitated nanoparticle. *Phys. Rev. Res.* **5**(3), 033101 (2023)
58. L. Dania, D.S. Bykov, F. Goschin, M. Teller, T.E. Northup, Northup, Ultra-high quality factor of a levitated nanomechanical oscillator. *Phys. Rev. Lett.* **132**(13), 133602 (2023)
59. J. Millen, T.S. Monteiro, R. Pettit, A.N. Vamivakas, Optomechanics with levitated particles. *Rep. Prog. Phys.* **83**(2), 026401 (2020)
60. T. Li, *Fundamental tests of physics with optically trapped microspheres* (Springer, New York, 2013)
61. A.S. Kuznetsov, K. Biermann, A.A. Reynoso, A. Fainstein, P.V. Santos, Micro-cavity phononitons—a coherent optical-to-microwave interface. *Nat. Commun.* **14**(1), 5470 (2023)
62. R.J. Glauber, *Quantum theory of optical coherence* (Wiley-VCH, Weinheim, 2006)
63. Y. Hu et al., Generation of optical frequency comb via giant optomechanical oscillation. *Phys. Rev. Lett.* **127**(13), 134301 (2021)
64. H. Stokowski et al., Integrated frequency-modulated optical parametric oscillator. *Nature* **627**(8002), 95–100 (2024)
65. J. Sheng, X. Wei, C. Yang, H. Wu, Self-organized synchronization of phonon laser. *Phys. Rev. Lett.* **124**(5), 053604 (2020)
66. Q. Xu et al., Tunable mechanical-mode coupling based on nanobeam-double optomechanical cavities. *Photonics Res.* **10**(8), 1819–1827 (2022)
67. A. Zivari et al., On-chip distribution of quantum information using traveling phonons. *Sci. Adv.* **8**(46), 2375–2548 (2022)
68. X. Hu, F. Nori, Phonon squeezed states generated by second-order raman scattering. *Phys. Rev. Lett.* **79**(23), 4605–4608 (1997)
69. T. Lu et al., Quantum squeezing induced nonreciprocal phonon laser. *Sci. China Phys. Mech. Astron.* **67**(6), 260312 (2024)
70. ‘Sound laser’ is the most powerful ever made. <https://www.newscientist.com/article/2421719-sound-laser-is-the-most-powerful-ever-made/>. Accessed 15 Mar 2024